NANO LETTERS

2009
Vol. 9, No. 4
1549-1554

Silicon Nanowire-Based Solar Cells on Glass: Synthesis, Optical Properties, and Cell Parameters

V. Sivakov,*,†,‡ G. Andrä,‡ A. Gawlik,‡ A. Berger,†,‡ J. Plentz,‡ F. Falk,‡ and S. H. Christiansen†,‡

Max Planck Institute of Microstructure Physics, Weinberg 2, D-06120 Halle, Germany, and Institute of Photonic Technology, Albert Einstein Strasse 9, D-07745 Jena, Germany

Received December 2, 2008; Revised Manuscript Received February 5, 2009

ABSTRACT

Silicon nanowire (SiNW)-based solar cells on glass substrates have been fabricated by wet electroless chemical etching (using silver nitrate and hydrofluoric acid) of 2.7 μm multicrystalline p^+nn^+ doped silicon layers thereby creating the nanowire structure. Low reflectance (<10%, at 300−800 nm) and a strong broadband optical absorption (>90% at 500 nm) have been measured. The highest open-circuit voltage (V_{oc}) and short-circuit current density (J_{sc}) for AM1.5 illumination were 450 mV and 40 mA/cm^2, respectively at a maximum power conversion efficiency of 4.4%.

In the past few years, there is an enormously growing interest in the development of thin film (2nd generation) solar cells on cheap, for example, glass substrates or even third generation (nanostructured materials with high efficiency and low cost) solar cell materials systems.[1] The variety of potential third generation solar cell material systems is uncounted although the silicon-based approaches are certainly favored due to materials abundance and nontoxicity at a high level of materials control and understanding together with a huge industrial infrastructure for low cost and high yield production. Feasible silicon based third generation solar cell approaches can base on silicon nanostructures such as silicon nanowires (SiNWs) also known as nanowhiskers which have gained much attention due to their unique physical properties and possible applications in the fields of nanoelectronics,[2−8] nanooptoelectronics,[8,9] nanophotovoltaics,[10−19] and for sensor applications.[20] The numerous simulations carried out by General Electric[21] and California Institute of Technology[22] research groups show that solar cells based on SiNWs have the potential to reach power conversion efficiencies up to 20%. When using the term SiNWs usually structures synthesized by the vapor−liquid−solid (VLS) growth mechanism[23] are meant that grow from the gas phase by supplying Si vapor (physical vapor deposition (PVD) methods such as molecular beam epitaxy (MBE)[24,25] or electron beam evaporation (EBE)[26,27]) or Si containing gases such as silane (SiH_4) (chemical vapor deposition (CVD)[28−30]) and catalyzing the one dimensionality of the growing nanostructure by a metal nanocatalyst droplet, for example, from gold that determines the diameter of the growing wire. When the growth is carried out on an oxide free Si wafer, the SiNWs can grow epitaxially; when growing on glass the SiNWs grow random in all sorts of different directions while keeping certain preferred growth directions. The challenge with the VLS method is multifold, for example, it is challenging to form high crystalline quality SiNWs with a predefined doping level or even with sharp axial p-n junctions. In direct comparison, the growth of sharp pn-junctions in alternating 2D layers with well-defined doping levels is easily to be obtained following completely understood processes. In a subsequent step, the formation of highly parallel SiNWs with desired lengths at diameters of the order of few ten nanometers up to a few hundred nanometers could easily be obtained by an aqueous electroless chemical etching of single crystalline silicon wafers.[31−36] For these etched SiNWs, some of the aforementioned challenges of VLS growth do not occur, for example, sharp doping profiles of choice can be realized in the initial wafer material for example, by epitaxial 2D layer deposition of doped homoepitaxial Si layers, the SiNW diameters and etching depth can be defined by the variation of etching time and/or etching solution. These wet chemically etched microcrystalline (mc)-Si surfaces show very low reflectance compared to Si thin layers or wafers.[15,37,38] This low reflectance is potentially interesting for photovoltaic applications where enough absorption of solar light in as thin

* To whom correspondence should be addressed. E-mail: vladimir.sivakov@ipht-jena.de or vladsiv@yahoo.com.
† Max Planck Institute of Microstructure Physics.
‡ Institute of Photonic Technology.

10.1021/nl803641f CCC: $40.75
Published on Web 03/12/2009

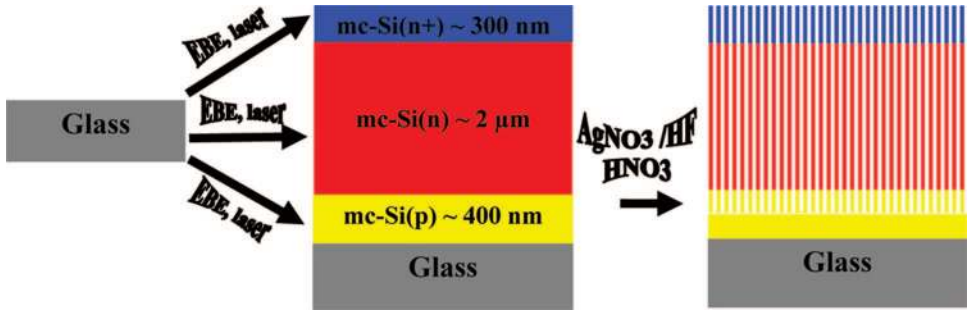

Figure 1. Schematic cross sectional view of the mc-Si p-n junction layer stack on a glass substrate (left) and the SiNWs after wet chemical etching (right).

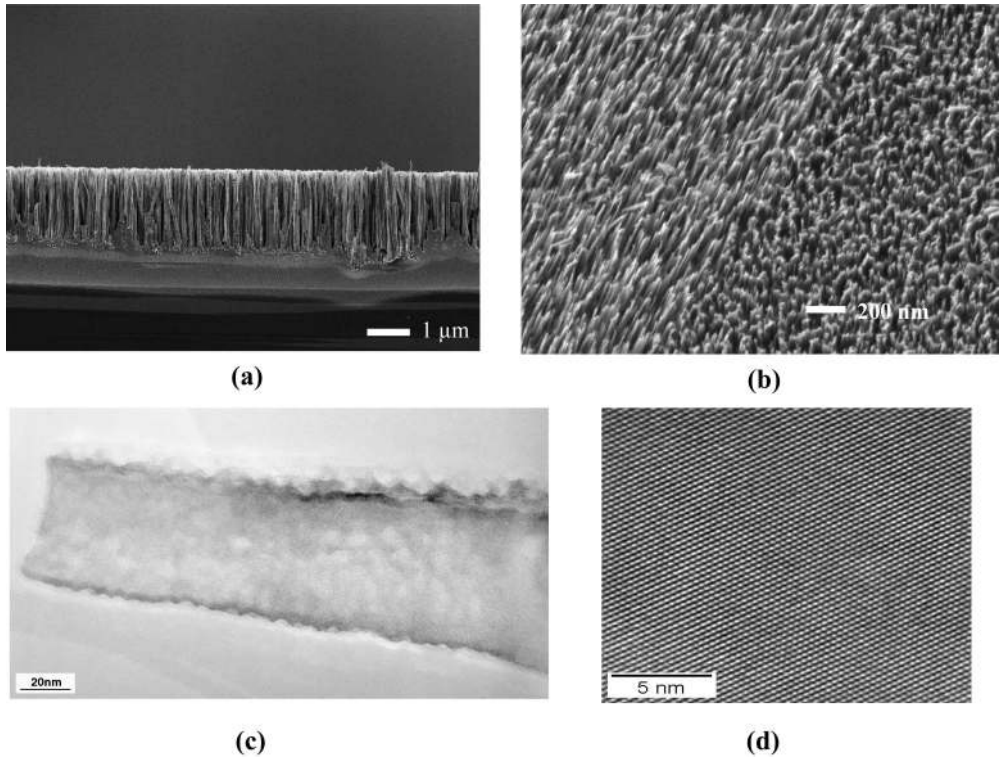

Figure 2. (a) Cross sectional SEM micrograph of the $AgNO_3$/HF etched mc-p^+nn^+-Si layer on glass. (b) Planar SEM micrograph of SiNWs etched into grains of different orientation; the grain boundary in the staring mc-Si layer is clearly discernible. (c) Bright-field TEM image of a segment of a SiNW. The rough SiNW sidewalls are clearly visible. (d) High resolution TEM image of the SiNW with the <111> lattice fringes clearly visible; the selected area is single crystalline.

as possible Si layer is desired and a combination of light trapping structures and antireflective coatings have usually to be applied.[19,37−39] The SiNWs themselves have shown to absorb solar light very satisfactorily and can therefore be used as the solar cell absorber.[21,39,40]

In this paper, we will show the wet chemical etching of SiNWs into a thin silicon layer on glass substrates to be useful to serve as a solar cell absorber in a thin film solar cell concept on glass. Solar cell parameters such as open circuit voltage (V_{oc}), fill factor (FF), efficiency (η), and short circuit current (I_{sc}) have been determined as well as structural and morphological appearance in transmission and scanning electron microscopy studies.

Figure 1 shows a schematic of the multicrystalline silicon layer stack on glass and the SiNW configuration after wet chemical etching.

Initially, a 200−400 nm thick amorphous Si (a-Si) layer is deposited by electron beam evaporation (EBE) at 200 °C deposition temperature on a borosilicate glass substrate (e.g., borofloat33 glass, www.schott.com) with a boron doping level of 5×10^{19} cm^{-3} (p^+). This layer is then crystallized by scanning the beam (beam shape/size: 0.8×0.3 mm^2) of a high power diode laser (806 nm wavelength, ROFIN SINAR DLX70S) at a power density of 10 kW/cm^2 and a scanning speed of 3.3 cm/s over the a-Si layer (which is heated to >520 °C for stress relief reasons) thereby crystallizing the a-Si while forming comparably large Si grains (of the order of a few ten micrometers) on the glass substrates.[41,42] On top of this seed layer, a 2 μm thick a-Si(n) phosphorus doped layer (phosphorus 6×10^{16} cm^{-3}) is deposited, again by EBE at 600 °C followed by a 300 nm a-Si(n^+) highly phosphorus doped layer (phosphorus 5 ×

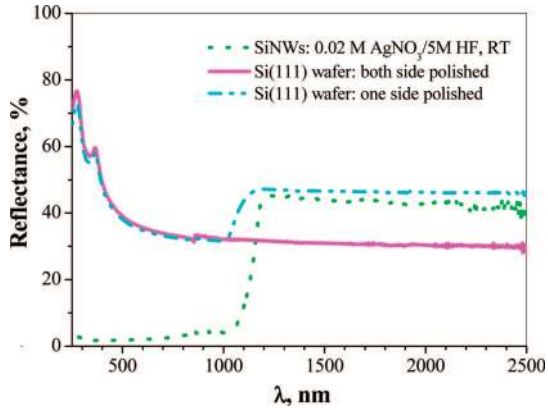

Figure 3. Reflectance spectra of SiNWs prepared via $AgNO_3$/HF etching of mc-p^+nn^+-Si layers on glass; as a reference, single or double side polished single crystalline silicon wafers were used.

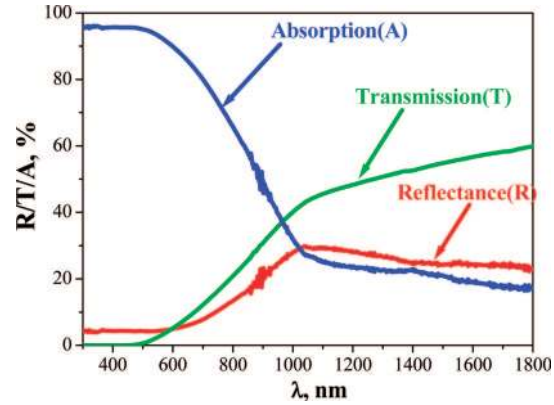

Figure 4. Optical transmission (T), reflectance (R), and absorption ($A = 1 - T - R$) of SiNWs prepared by etching of ~2.7 μm thick mc-p^+nn^+-Si layers on glass.

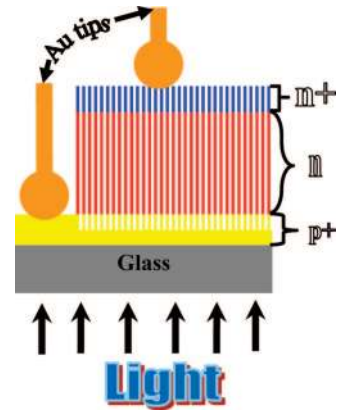

Figure 5. Schematic representation of the $I-V$ curve measurements of SiNW based p-n junctions.

10^{19} cm^{-3}). These layers were epitaxially crystallized by laser crystallization using an excimer laser (Lambda Physik LPX300, $\lambda = 248$ nm, 25 ns pulse duration, 600 mJ/cm^2 fluence).[41,42] In this process, only small portions of the material (~30 nm thick layers) are deposited at a time that can well be crystallized in a single excimer laser shot. That is, the 2 μm n-Si with a phosphorus doping level of 6×10^{16} cm^{-3} and the 300 nm n^+-Si with a phosphorus doping level of 5×10^{19} cm^{-3} layers are deposited by EBE in ~80 steps (duration of the crystallization of the entire layer stack takes ~20 min for an area of 25 × 25 mm). As a result of this epitaxial thickening, we obtain a large grained 2.5−3 μm thick silicon layer on glass substrates with the grain size and grain boundary population given by the diode laser seed layer crystallization.[41,42]

The SiNWs are then realized in the 2.5−3 μm thick mc-Si layer by electroless etching.[31−36] The desired p-n junction layout has been realized already in the thin film layer stack on glass prior to wet chemical etching. Our solar cell concept is based on a p^+nn^+-Si junction stack on glass. For the etching procedure, a mixture of 0.02 M silver nitrate ($AgNO_3$) and 5 M hydrofluoric acid (HF) in the volume ration 1:1 was used. The etching process is based on the galvanic displacement of silicon thereby oxidizing the silicon so that the HF can remove the silicon oxide and in parallel by reducing the silver (I) to metallic silver (0) at the mc-Si surface. The mc-Si layers of all in all ~3 μm thickness were completely etched at room temperature within ~30 min. Structural analysis of the etched SiNWs has been carried out by field emission scanning electron microscopy (FESEM, JEOL JSM-6300F) and high resolution transmission electron microscopy (HRTEM, FEI CM200/UT). Optical characterization has been carried out in a UV−VIS/NIR spectrometer (Perkin-Elmer Lambda 900) equipped with a 150 mm integrating sphere. Respective transmission (T) and reflectance (R) spectra were measured and a net internal absorption (A) has been calculated according to $R + T + A = 1$. $I-V$-curves under illumination of the SiNW-based solar cell are measured using a sun simulator (AM1.5, 1000 W/m^2, SS-80 PET). Laser beam-induced current (LBIC) measurements are performed with a Helium−Neon laser (wavelength 633 nm, spot size 100 μm) and a 2D scan unit (25 × 25 μm^2 reading points). During the scan the photocurrent in each illuminated spot is detected by a sensitive amperemeter (Keithley 236). Illumination is carried out through the glass substrate.

Figure 2 shows scanning electron microscopy (SEM) and transmission electron microscopy (TEM) micrographs of the SiNWs after wet chemical etching into the mc-p^+nn^+-Si layers on glass. Figure 2a shows an SEM micrograph of SiNWs in cross section. The etching profile is homogeneous and the etching depth approximately is 2.3−2.5 μm from the top surface. Figure 2b shows an SEM micrograph of SiNWs from the top surface. A difference in the SiNW orientation is discernible for starting grains of different orientation prior to wet chemical etching. The diameter of the SiNWs varies from 20 to 100 nm with an average of approximately 35 nm, as measured from TEM investigations (a typical example is given in Figure 2c). SiNWs are single crystalline as shown in the high-resolution TEM image in Figure 2d, although they possess a comparably large surface roughness. The mean roughness of these nanowires varies from wire to wire, but stays typically in the range of 1−5 nm with a roughness period of the order of several nanometers.

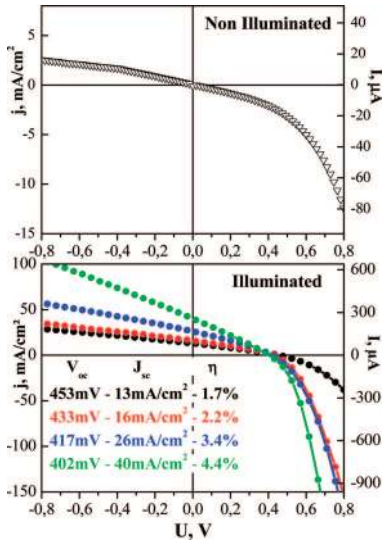

Figure 6. Nonilluminated and illuminated (AM1.5) $I-V$ curves of SiNWs etched into a mc-p^+nn^+-Si layer on glass. SiNW are irradiated through the glass substrate (superstate configuration) and contacted by metal tips at four different sample positions. The right-hand scale gives real measured current values and the left-hand scale current density values.

The optical reflectance spectra of $AgNO_3$/HF etched mc-p^+nn^+-Si surface on glass and single crystalline wafers are shown in Figure 3. The average reflectance of SiNWs realized by wet chemical etching is less than 5% within a range of wavelengths between 300 and 1000 nm. The reflectance values (R) are much smaller than those of a polished Si wafer (that shows an R of more than 30%).

The absorption (A) of SiNWs on glass was determined from the optical reflectance (R) and transmission (T) measurements as shown in Figure 4. The SiNWs show a very low reflectance as was also pointed out in Figure 3. In the last several years, in many reports it could be shown that Si nanostructures can be used as antireflective coatings in solar cells.[21,38−40] Our observation shows the same tendency. On the other hand, it has to be stated that the SiNWs do not transmit light in the range between 300 and 550 nm. This transmission would however be important to use them as antireflection coating on top of a processed solar cell. Moreover, the absorption of the 2.7 μm mc-Si layers with etched nanowire structures at wavelength >550 nm was observed to be higher than that of a Si layer of the same thickness. These optical phenomena are selling propositions for the realization of efficient solar cells based on etched SiNWs.

To characterize the optoelectronic properties of SiNWs, they were contacted by metallic tips in initial experiments. As shown in Figure 5, a gold tip (450 μm in radius as measured by SEM and optical microscopy) was brought in contact with the surface of the SiNWs. Another tip was placed on the diode laser crystallized p^+-seed layer in close vicinity. The samples were illuminated through the glass substrate using well defined AM1.5 illumination conditions. $I-V$ curves are shown in Figure 6. The four different curves were obtained at different positions within a single sample. While in all cases the open circuit voltage (V_{oc}) is rather similar lying in the range of 410−450 mV, the short circuit current (I_{sc}) values differ appreciably. This may be due to the point contacting with gold needles that allows either to contact a higher or lower number of SiNWs just depending on position. Therefore, it is not so easy to give a reliable current density. The short circuit current densities, j_{sc}, in Figure 6 ranging from 13.4 to 40.3 mA/cm^2 were calculated from the measured current and the maximum area to be contacted by our metal tip of 0.64 mm^2 cross sectional area at a radius of ~450 μm. Only those carriers contribute to the current that is generated in SiNWs that stay in contact with the metal tip. $I-V$ curves in Figure 6 show a strong deviation from the ideal almost square shape of the curve, as given by a large slope (approaching infinity) parallel to the y-axis and a small slope (going to zero) parallel to the

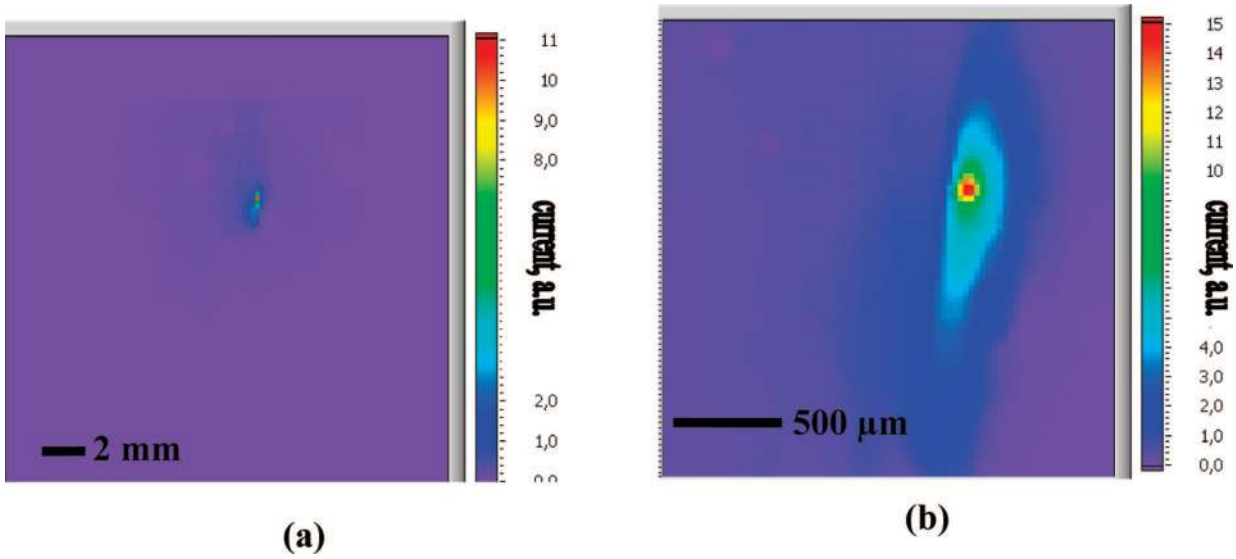

Figure 7. Laser beam induced current maps of SiNW based solar cells contacted by a metal tip. (a) 20 × 20 mm area, (b) 2 × 2 mm region around the contacting metal tip.

x-axis. Severe shunting is responsible for the deviation of the $I-V$-curve parallel to the *y*-axis; a large series resistance is responsible for a deviation of the curve parallel to the *x*-axis. Shunting may be due to the large unpassivated surface of the SiNWs or even due to surface currents along the SiNW surfaces. A high contact resistance is probably a result of just lowering the metal tip to the SiNW surfaces and is responsible for a large series resistance. High series resistance and shunting lead to a low fill factor FF of about 30%. From the measured values an energy conversion efficiency (η) of 1.7 to 4.4% follows. To get a more reliable size determination of the contacted area that in turn contributes to the measured current, laser beam-induced current (LBIC) measurements were carried out. Figure 7 shows the results of LBIC taken from the total area of about 20 × 20 mm (Figure 7a) and from a region around the contacting metal tip (Figure 7b). From Figure 7a, it follows that photo current is induced from illuminating a 1 × 2 mm^2 large area around the contact tip. This area is three times the contact area itself. Therefore we conclude that by a light-trapping effect light from the surroundings is scattered into the region of contacted SiNWs to generate current there. The anisotropy of light diffusion obvious from Figure 7 could be due to the anisotropy of the SiNW morphology as shown in Figure 2b. Figure 7b shows that even within the region of contacted SiNWs the current density is rather inhomogeneous, which might be due to differences in the contact resistance of different nanowires. If one assumes an area of 2 mm^2 contributing to the current of Figure 6 then the current density and the efficiency reduce to ~13 mA/cm^2 and 1.4%, respectively. However, current densities higher than 10% of the maximum value come from an area of only less than 1 mm^2 around the tip as is obvious from Figure 7b. Therefore the current density and efficiency values given in Figure 6 are more real than those calculated from a current gathering area of 2 mm^2.

In conclusion, we have produced a solar cell based on SiNWs on glass substrates using an electroless wet chemical etching process of a mc-p^+nn^+-Si layer on glass. Optical and photovoltaic properties of such nanostructures on glass were investigated. The highest obtained open-circuit voltage (V_{oc}) under AM 1.5 illumination was 450 mV. Under these conditions a short-circuit current of 0.25 mA was measured by contacting with a metal tip of 450 μm radius. Depending on the area to be used current densities between 13 mA/cm^2 (area from which light is gathered) to 40 mA/cm^2 (area of metal tip) follow. This leads to efficiencies in the 1.4−4.4% range. The highest power conversion efficiency of SiNWs based solar cell on glass was 4.4% that shows potential for low cost solar cells with such design. Nevertheless, the high current density of about 40 mA/cm^2 requires complete light absorption and high quantum efficiency. It has to be investigated how well laser beam induced current (LBIC) measurements with a small illuminated area and $I-V$ measurements with a large illuminated area fit together. However, the rather large values of the current densities have to be confirmed by measurements performed using large area contacts instead of metal tips. To this end, appropriate contacting schemes have to be developed. Moreover, to increase the power conversion efficiency for such nanostructures, the shunting has to be minimized and all production steps must be optimized.

Acknowledgment. The authors thank Dr. E. Ose and Mrs. A. Schumann for seed layer preparation. V.S. thanks Dr. G. Sarau and Dr. Th. Stelzner for fruitful discussions. Preparation of samples for TEM investigations by Mrs. S. Hopfe (Max Planck Institute of Microstructure Physics, Halle/Germany) is gratefully acknowledged. The authors gratefully acknowledge the German Science Foundation (DFG, Contract No. CH-159/1) for supporting this work.

References

(1) Green, M. A. *Proceedings IEEE 4th World Conference on Photovoltaic Energy Conversion*, Waikoloa, HI, May 7–12, **2006**, *1*, 15.
(2) Duan, X.; Lieber, C. M. *Adv. Mater.* **2001**, *12*, 298.
(3) Gudiksen, M. S.; Wang, J.; Lieber, C. M. *J. Phys. Chem. B* **2001**, *105*, 4062.
(4) Cui, Y.; Duan, X.; Hu, J.; Lieber, C. M. *J. Phys. Chem. B* **2000**, *104*, 5213.
(5) Duan, X.; Huang, Y.; Cui, Y.; Wang, J.; Lieber, C. M. *Nature* **2001**, *409*, 66.
(6) Cui, Y.; Lieber, C. M. *Science* **2001**, *291*, 851.
(7) Huang, Y.; Duan, X.; Cui, Y.; Lauhon, L.; Kim, K.; Lieber, C. M. *Science* **2001**, *294*, 1313.
(8) Huang, Y.; Duan, X.; Lieber, C. M. *Small* **2005**, *1*, 142.
(9) Duan, X.; Huang, Y.; Argarawal, R.; Lieber, C. M. *Nature* **2003**, *421*, 241.
(10) Lu, W.; Lieber, C. M. *J. Phys. D: Appl. Phys.* **2006**, *39*, R387.
(11) Muskens, O. L.; Rivas, J. G.; Algra, R. E.; Bakkers, M.; Lagendijk, A. *Nano Lett.* **2008**, *8* (9), 2638.
(12) Kelzenberg, M. D.; Turner-Evans, D. B.; Kayes, B. M.; Filler, M. A.; Putnam, M. C.; Lewis, N. S.; Atwater, H. A. *Nano Lett.* **2008**, *8* (2), 710.
(13) Fang, H.; Li, X.; Song, S.; Xu, Y.; Zhu, J. *Nanotechnology* **2008**, *19*, 255703.
(14) Hu, L.; Chen, G. *Nano Lett.* **2007**, *7* (11), 3249.
(15) Stelzner, Th.; Pietsch, M.; Andrä, G.; Falk, F.; Ose, E.; Christiansen, S. H. *Nanotechnology* **2008**, *19*, 295203.
(16) Tian, B.; Zheng, X.; Kempa1, T. J.; Fang, Y.; Yu, N.; Yu, G.; Huang, J.; Lieber, C. M. *Nature* **2007**, *449*, 885.
(17) Yang, C.; Zhong, Z.; Lieber, C. M. *Science* **2005**, *310*, 1304.
(18) Peng, K.; Huang, Z.; Zhu, J. *Adv. Mater.* **2004**, *16*, 73.
(19) Peng, K.; Xu, Y.; Wu, Y.; Yan, Y.; Lee, S. T.; Zhu, J. *Small* **2005**, *1*, 1062.
(20) Elibol, O. H.; Morisette, D.; Akin, D.; Denton, J. P.; Bashir, R. *Appl. Phys. Lett.* **2003**, *83*, 4613.
(21) Tsakalakos, L.; Balch, J.; Fronheiser, J.; Korevaar, A.; Sulima, O.; Rand, J. *Appl. Phys. Lett.* **2007**, *91*, 233117.
(22) Kayes, B. M.; Lewis, N. S.; Atwater, H. A. *J. Appl. Phys.* **2005**, *97*, 114302.
(23) Wagner, R. S.; Ellis, W. C. *Appl. Phys. Lett.* **1964**, *4*, 89.
(24) Schubert, L.; Werner, P.; Zakharov, N. D.; Gerth, G.; Kolb, F. M.; Long, L.; Tan, T. Y.; Gösele, U. *Appl. Phys. Lett.* **2004**, *84*, 4968.
(25) Zakharov, N. D.; Werner, P.; Gerth, G.; Schubert, L.; Sokolov, L.; Gösele, U. *J. Cryst. Growth* **2006**, *290*, 6.
(26) Sivakov, V.; Heyroth, F.; Falk, F.; Andrä, G.; Christiansen, S. H. *J. Cryst. Growth* **2007**, *300*, 288.
(27) Sivakov, V.; Andrä, G.; Himcinschi, C.; Gösele, U.; Zahn, D. R. T.; Christiansen, S. *Appl. Phys. A* **2006**, *85*, 311.
(28) Schmidt, V.; Senz, S.; Gösele, U. *Appl. Phys. A* **2005**, *80*, 45.
(29) Schmidt, V.; Senz, S.; Gösele, U. *Nano Lett.* **2005**, *5*, 931.
(30) Hochbaum, A. I.; Fan, R.; He, R.; Yang, P. *Nano Lett.* **2005**, *5*, 457.
(31) Peng, K. Q.; Yan, Y. J.; Gao, S. P.; Zhu, J. *Adv. Mater.* **2002**, *14*, 1164.
(32) Huang, Z.; Zhang, X.; Reiche, M.; Liu, L.; Lee, W.; Shimizu, T.; Senz, S.; Gösele, U. *Nano Lett.* **2008**, *8* (9), 3046.
(33) Peng, K. Q.; Wu, Y.; Fang, H.; Zhong, X. Y.; Xu, Y.; Zhu, J. *Angew. Chem., Int. Ed.* **2005**, *44*, 2737.
(34) Peng, K. Q.; Hu, J. J.; Yan, Y. J.; Wu, Y.; Fang, H.; Xu, Y.; Lee, S. T.; Zhu, J. *Adv. Funct. Mater.* **2006**, *16*, 387.
(35) Qiu, T.; Wu, X. L.; Yang, X.; Huang, G. S.; Zhang, Z. Y. *Appl. Phys. Lett.* **2005**, *84*, 386.

(36) Peng, K.; Zhang, M.; Lu, A.; Wong, N. B.; Zhang, R.; Lee, S. T. *Appl. Phys. Lett.* **2007**, *90*, 163123.
(37) Andrä, G.; Pietsch, M.; Stelzner, Th.; Falk, F.; Christiansen, S. H.; Scheffel, A.; Grimm, S. *Proceedings 22nd European Photovoltaic Solar Energy Conference and Exhibition*, Milan, Italy, September 3–7, **2007**, 481.
(38) Andrä, G.; Pietsch, M.; Sivakov, V.; Stelzner, Th.; Gawlik, A.; Christiansen, S.; Falk, F. *Proceedings 23nd European Photovoltaic Solar Energy Conference and Exhibition*, Valencia, Spain, September 1–5, **2008**, 163.
(39) Tsakalakos, L.; Balch, J.; Fronheiser, J.; Shih, M. Y.; LeBoeuf, S. F.; Pietrzykowski, M.; Codella, P. J.; Korevaar, B. A.; Sulima, O.; Rand, J.; Davuluru, A.; Rapol, U. *J. Nanophoton.* **2007**, *1*, 013552.
(40) Koynov, S.; Brandt, M. S.; Stutzmann, M. *Appl. Phys. Lett.* **2006**, *88*, 203107.
(41) Falk, F.; Andrä, G. EU Patent EP1,314,208 B1, May 28th, 2003.
(42) Falk, F.; Andrä, G. U.S. Patent 7,091,411 B2, Aug. 15th, 2006.

NL803641F